ANL/ET/CP-99592

SURFACE AND INTERFACE MODIFICATION SCIENCE AND TECHNOLOGY*

J.-H. Park
Argonne National Laboratory, Argonne, IL 60439, U. S. A.
jhpark@anl.gov, Tel: (630)252-5104, Fax: (630)252-3604

June 1999

INVITED presentation in the session on Environmentally Sound Material Technology Development of 1999 World Korean Scientists and Engineers Symposium, Seoul, Korea July 6-16, 1999

* Work supported by the U.S. Department of Energy, under Contract W-31-109-Eng-38.

DISCLAIMER

SURFACE AND INTERFACE MODIFICATION SCIENCE AND TECHNOLOGY

J.-H. Park
Argonne National Laboratory, Argonne, IL 60439, U. S. A.
jhpark@anl.gov, Tel: (630)252-5104, Fax: (630)252-3604

Surface modification of solids is of scientific and technological interest due to its significant benefits in a wide variety of applications. Various coatings applications such as corrosion protection and electrical insulators and conductors are required for proper engineering design based on geometrical relationships between interfaces and on thermodynamic/kinetic considerations for the development of surface modifications. This paper will explore three basic examples: the proton conductor $BaCeO_3$, high-temperature protective coatings, and epitaxial relationships between interfaces.

INTRODUCTION

Coating for use as surface modification, such as those for corrosion protection and for electrical insulation and conduction and conductors, are of great technological and scientific interest because of their significant benefits over a broad range of applications. Such coatings must be developed on the basis of the geometrical relationships of the interfaces between the coatings and the substrates, as well as on thermodynamic/kinetic considerations. For example, surfaces are typically subjected to adsorption and reaction phenomena such as physical and or chemical deposition, corrosion, and catalytic reactions. This paper examines basic examples of surface modification with the proton-conducting $BaCeO_3$ and high-temperature protective coatings, as well as the epitaxial relationships at interfaces.

1 Proton-Conducting Perovskite Oxide, $BaCeO_3$

We would like to demonstrate the principles of both thermodynamic and kinetic aspect for the surface incorporation of the most common environmental reactive chemical species, i.e., CO_2 and H_2O, with the proton-conducting perovskite oxide, $BaCeO_3$.[1]

1.1 Thermodynamic aspect

We can consider the stability of $BaCeO_3$ in CO_2 and H_2O environments:[2,3]

$$BaCeO_3 + CO_2 = BaCO_3 + CeO_2 \quad (1)$$

$$BaCeO_3 + H_2O = Ba(OH)_2 + CeO_2. \quad (2)$$

Under equilibrium conditions, the equilibrium partial pressures of CO_2 and water vapor are defined by the reactions

$$pCO_2 = \exp(\Delta G^\circ_{BaCO_3}/RT) \quad (3)$$

and

$$pH_2O = \exp(\Delta G^\circ_{Ba(OH)_2}/RT), \quad (4)$$

where $\Delta G^{\circ}_{BaCO_3}$ and $\Delta G^{\circ}_{Ba(OH)_2}$ are the standard Gibbs free energies of formation of the $BaCO_3$ and $Ba(OH)_2$, respectively, in Eqs. 1 and 2. From Eqs. 3 and 4, it appears that one should be able to deduce the conditions for caborization or hydration; however, a further reaction must be considered, namely

$$BaCO_3 + H_2O = Ba(OH)_2 + CO_2, \quad (5)$$

with equilibrium condition

$$(pCO_2 / pH_2O)_{eq} = \exp [(\Delta G^{\circ}_{BaCO_3} - \Delta G^{\circ}_{Ba(OH)_2})/RT], \quad (6)$$

when the unity activity for the solid phases. Examination of Eqs. 3, 4, and 6 permits the identification of various situations that the type of surface correction products can be formed, as follows:

(i) If both gas-phase pCO_2 and pH_2O are lower than those of the equilibrium partial pressures, then $BaCeO_3$ is stable;

(ii) If gas-phase $pCO_2 < pCO_2$ (equal), and gas-phase $pH_2O > pH_2O$(equal), then $Ba(OH)_2$ is the only stable phase;

(iii) If gas-phase $pCO_2 > pCO_2$ (equal), and gas-phase $pH_2O < pH_2O$(equal), then $BaCO_3$ is the only stable phase;

(iv) If gas-phase $pCO_2 > pCO_2$ (equal), and gas-phase $pH_2O > pH_2O$(equal), then both $Ba(OH)_2$ and $BaCO_3$ should be stable and will form as surface products.

However, reference to Eq. 6 indicates that only one phase will form, depending on which of the following two conditions prevails:

(a) $(pCO_2 / pH_2O)_{gas} > (pCO_2 / pH_2O)_{eq}$:

This condition will cause Reaction 5 to proceed to the left, and $BaCO_3$ will be the stable phase where the $BaCeO_3$ is in contact with gas phase.

(b) $(pCO_2 / pH_2O)_{gas} < (pCO_2 / pH_2O)_{eq}$:

This condition will cause Reaction 5 to proceed to the right, and $Ba(OH)_2$ will be the stable phase where the $BaCeO_3$ is in contact with gas phase. We can represent the possible reaction product as a function of gas chemistry in order to construct a thermochemical diagram that depicts the stability range of various condensed phases as functions of the thermodynamic activities of the two components of reactive gas, such as CO_2 and H_2O in air, etc. Based on the above analysis, we can build the thermochemical diagram for $BaCeO_3$ and $BaCO_3$ and $Ba(OH)_2$ at 900K by using literature values reported in Ref. 2 as a function of pCO_2 and pH_2O (see Fig. 1).

1.2 Kinetic aspects:

In Fig. 1, one sees that proposed reactions 1, 2, and 5 will be applied to evaluate thermodynamic stability; however, this will be reconsidered when the kinetics are hindered by the sluggish solid-state diffusion process, such as oxidation of metals, (e.g.,

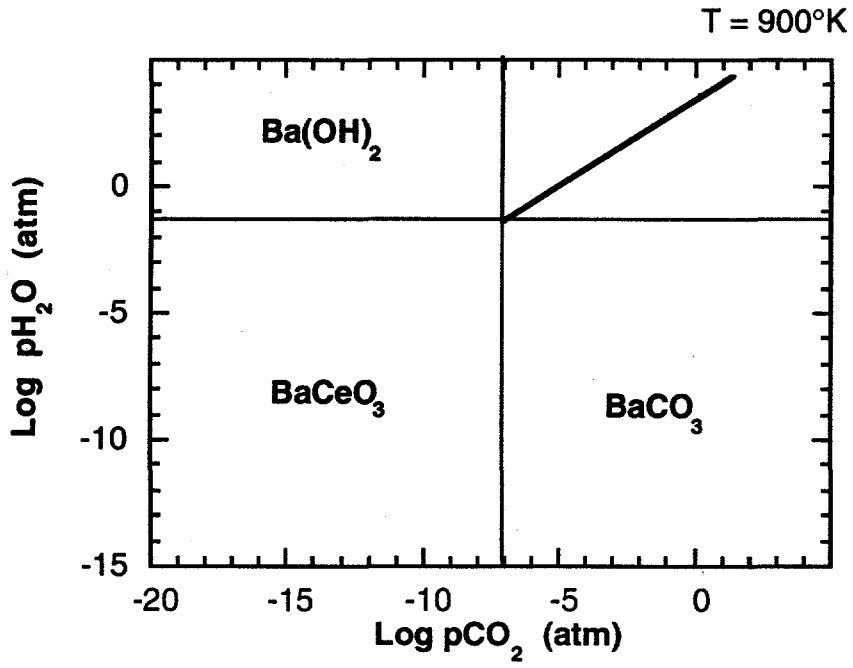

Fig. 1.
Thermochemical diagram for H_2O-CO_2-$BaCeO_3$ system at 900K.

presence of very thin aluminum oxide scale on the aluminum.) Figure 2 shows the $BaCeO_3$ perovskite ceramic surface exposed to H_2O and CO_2 environments. Eventually CO_2 will be reacted only at the surface to form a monolayer of -CO_2, via chemical reaction and/or chemical (Ad/de)sorption. The result of CO_2 incorporation at the $BaCeO_3$ surface could be explained as $BaCeO_3$ surface blocking by CO_2 at the surface: for the continuous reaction, Ba ions should be extruded to the surface. However, Ba ion diffusivity in the $BaCeO_3$ is expected to be extremely low, and therefore mostly CO_2 will be interacted at the surface only. However, protons from water will be diffused into the bulk $BaCeO_3$, depending on chemical potential gradient.

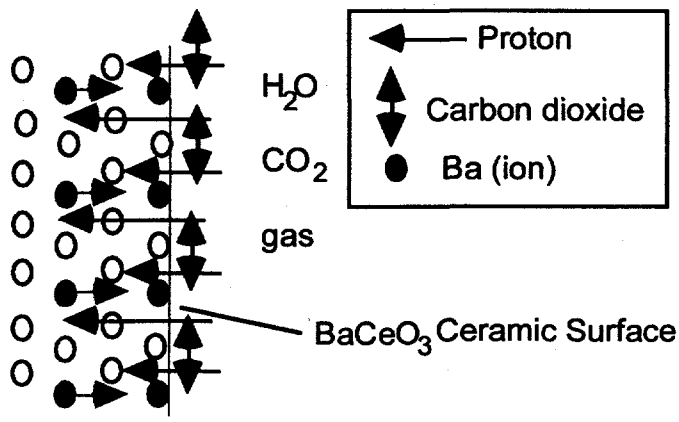

Fig. 2.
$BaCeO_3$ ceramic surface exposed to H_2O and CO_2 environments.

2 High-Temperature Chemical Vapor Deposition (CVD)

The key issues of fundamental and technological approaches of high-temperature thermal CVD film technology on the solid–state interactions between calcium vapor and oxygen in vanadium alloys were investigated.[4] The near–surface region of the specimens was charged with oxygen or a 1% CO-CO_2 gas mixture or air to form vanadium oxide. The specimens were placed above a calcium vapor source in a Knudsen sublimation cell. Calcium reacts with the oxygen–precharged surface and diffuses through the CaO or Ca–V_XO_Y layer, as shown in Fig. 3. Reactions for the formation of the coatings are

$$\text{Ca (vapor)} + \underline{O}\text{ (alloy)} = \text{CaO} \tag{7}$$

and

$$\text{Ca (vapor)} + V_XO_Y\text{ (alloy surface)} = CaV_XO_Y, \tag{8}$$

where $\underline{O}$ represents oxygen activity at the interface between the CaO and the oxygen–charged vanadium alloy. These reactions occur spontaneously, and the rate–determining step is most likely ionic diffusion (Ca^{+2}) through the CaO layer. The X-ray diffraction spectrum of the CaO coating on V-alloys clearly showed the two sets of peaks for CaO and V-alloy and indicated no other phases. The X-ray beam can penetrate ≈40 μm into CaO, and into a normal film thickness of ≈3 μm; the spectrum of the V-alloy substrate is also present.

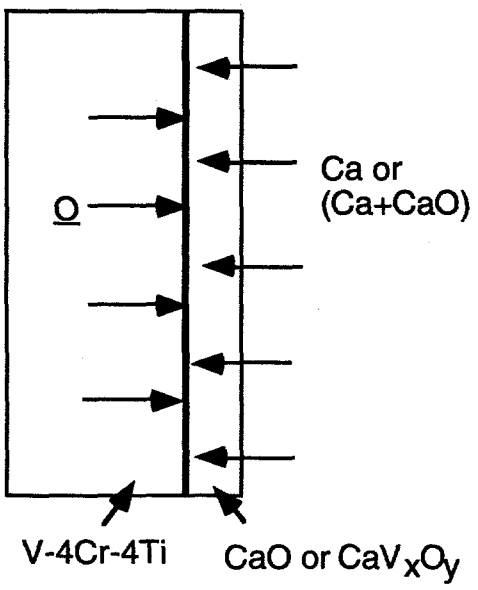

Fig. 3.
Schematic diagram of solid–state reaction steps at V–alloy/CaO interface: initial reaction is Ca + O = CaO.

Sublimation of calcium in a relatively low vacuum of 10^{-4}–10^{-5} torr, when oxygen was present as an impurity, enabled the formation of CaO clusters by oxidation of calcium vapor inside the chamber. After coating the V–alloy specimens at 800 or 850°C for electrical resistance measurements, the system was cooled to room temperature while purging with 99.999% argon. In one experiment, the calcium reservoir was raised to the top of the furnace (cool region) and the specimens held at temperature for 3–5 h to determine if additional oxidation occurred. No appreciable weight gain or loss was detected after CaO had been deposited. To determine the electrical resistance of the

coatings and also facilitate SEM/EDS analysis, the samples were coated with gold by sputter-deposition of an array of ≈1–mm-diameter discs on the surface of the coatings. The discs, when placed in contact with gold foil, provided a good electrical connection over a large area of the specimen. Ohmic resistance was measured at 25–500°C in air. Only the specimen charged with oxygen in 99.999% argon and coated with calcium by CVD exhibited insulator behavior. The specimens oxidized in air and in a 1% CO-CO_2 gas mixture and coated by CVD showed semiconductor behavior.

3 Protective coatings

Corrosion resistance of structural iron-based alloys in high-temperature environments is typically achieved by formation of a continuous protective oxide scales such as chromium oxide or aluminum oxide, which acts as a diffusion barrier between the environment and the alloys. Such coatings may cover the alloy surface only superficially and are subject to erosion or spallation under severe high-temperature conditions. Two fundamental goals that must be addressed in the development of more oxidation-resistant alloys are to (a) decrease the transport rate of metal ions and/or oxygen through the scale, and (b) improve scale adhesion to the alloy substrate.
The use of "reactive elements" (e.g., yttrium, lanthanum, cerium) in alloys influences the properties of both the scale[5] and the alloy substrate during high-temperature oxidation. Alloys without oxygen-active elements exhibit outward cation migration during oxidation. However, when the reactive elements are present in the alloy, inward anion transport predominates during scale growth.[6,7] The reactive elements tend to inhibit grain growth, i.e., they stabilize the alloy substrate during high-temperature oxidation. Our work showed that reactive elements in Fe-Cr alloys inhibit grain growth in the alloy and suppress Fe diffusion through the scale.[8] Transmission electron microscopy (TEM) and scanning electron microscopy (SEM) confirmed the grain-boundary segregation of the stable intermetallic phases[6,8] (See schematic drawing in Fig. 4).

3.1 Diffusion approach

It has been generally reported that the addition of ≈1% of the so-called reactive elements to the alloys decreases the rate of scale growth and enhances scale adhesion. Grain-boundary transport could be the main contribution in high-temperature chromia-forming oxidation; therefore, measurements were made of bulk, dislocation, and grain-boundary diffusion of cations and anions in pure and Y-doped Cr_2O_3. Chromia is thought to grow via outward diffusion of cations from the metal to the oxide/gas interface. When the scale formation proceeds by diffusion along short-circuit paths like grain boundaries in the oxide layer, the equation that describes the usual diffusion-controlled oxidation kinetics is

$$x^2 = k_p t, \tag{9}$$

where x is the oxide thickness, t is time, and k_p is the so-called parabolic rate constant, the expression for k_p must be modified to reflect the fact that grain-boundary diffusion is the dominant mechanism of mass transport in the scale.

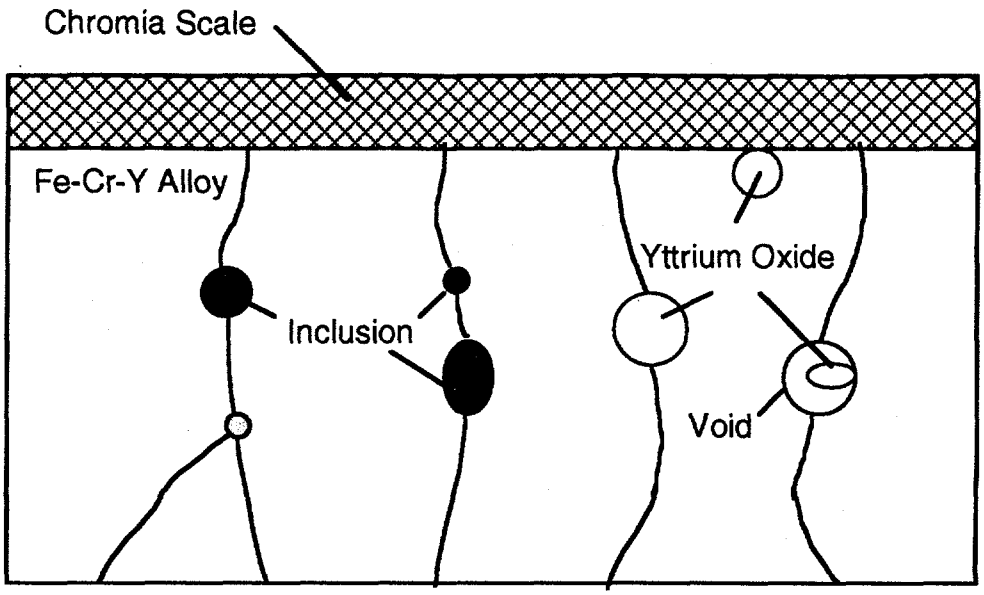

Fig. 4
Grain-growth inhibition by inclusion (Fe-Cr-Y), and Y_2O_3 segregated in alloy grain boundaries.

This assumption could be applicable only if no open voids or microcracks are present in the scale or the perfect match between oxide scale and the alloy interfaces. However, real oxidation may not be matched with the assumption considered. Several research groups have demonstrated that bulk diffusion of cations as measured in chromia single crystals and polycrystals are to slow to explain observed rates of oxidation in alloys that form chromium oxide layer. The calculated oxidation rate based on grain-boundary diffusivity is still 10 times too low to account for the measured oxidation rates (e.g., Cr, Cr-Y, Fe-25Cr, and Fe-25Cr-[Ce, or Y], etc., Ce, Y = 0.1-3 wt.%)[9]. This presumably tells us that other important mechanisms should be considered, e.g., a dynamic situation may increase the mass transport rate during chromia-forming oxidation. This question remains *unresolved*, but the cause could be *surface diffusion* near the wide-open grain boundaries generated, or vapor phase transport near the interfaces of alloy to the scale based on a dynamic situation during high-temperature scale growth and may be improperly compared with the chromia ceramic grain-boundary diffusion data with naturally forming grain-boundaries. According to our observation of grain-boundary data, as-grown chromia scale in the chromium metal was identical with ceramic chromia, except as grown scale showed small microcracks due to the sample handling procedure. In alloys bearing reactive elements, inward diffusion of anions is the predominant process. In the case of Fe-Cr-Y alloys, no Fe diffused outward; however, when no Y was present in the alloys, Fe outward diffusion contributed to faster diffusion paths of FeO or Fe_3O_4 via fast channels in Cr_2O_3 scales.[9] Based on this anion inward diffusion during oxidation of commercially developed alloys, a more advanced concept for the surface modification on the high-temperature alloys was developed. To understand the directional diffusion process (either anion inward or cation outward for the oxidation process) is a very important for its development of surface modification by many different processes including high-temperature CVD.

3.2. Scale adhesion

Figure 5 shows schematic representations for two different diffusion processes.

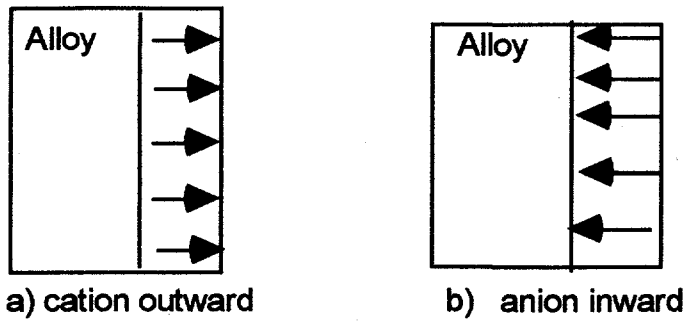

Fig. 5.
Schematic view for the two different diffusion process during alloy oxidation.

When reactive elements are present in an alloy, scale adhesion is generally good. The main considerations are (a) stability of alloy substrates during high-temperature oxidation and anion inward diffusion and (b) oxide formation at the scale/alloy interface as shown in Fig. 5. Some reactive elements (e.g., Y) provide both conditions satisfactorily, according to oxidation tests of Fe-Cr alloys with and without Y-containing alloys. The alloy bearing Y showed good scale adhesion, but that without Y showed total spallation or loose bonding at metal/scale interfaces. The most favorable behavior for Y was substrate stabilization during oxidation. According to the grain-growth behavior of the various Fe-Cr alloys without oxidation, Y (0.1-3 wt.%) provided the most stable alloy substrate. For Ce-bearing alloys (0.3-1 wt.%), most Ce was migrate to the specimen surface, and alloy grains became enlarged during annealing. However, preheated samples of Fe-25Cr did not show spallation; this could indicate that the stabilized-grain samples showed a higher degree of adhesion. On the other hand, longer oxidation times showed Fe outward diffusion, which caused the oxidation process to be more rapid than that of pure chromia-forming oxidation.[9]

4 Epitaxial relationship between layers

When we pursue the engineering applications for the epitaxial relationship between substrate and film, or between films, two main considerations are a) thermodynamics and b) lattice parameters with properly designed orientations so that the interface of interested in suitable for the process. As an example, when we deposit CeO_2 film on Ni by high-temperature, low-atmospheric-pressure CVD, environment should be met both CeO_2 and Ni stable conditions. Figure 6 shows the superimposed spectrums obtained by means of four cycled-X-ray diffraction that applied CeO_2 deposited by CVD on (200) textured Ni foil.[10] From the observations several results are applicable to engineering considerations. Figure 7 is a schematic orientational view of the CeO_2 deposit on the Ni. The lowest interface energy state between CeO_2 and Ni for both (200) could be 45°, which is consistent with Fig. 6. According to the literature, the X-ray lattice parameter for Ni (FCC, z = 4) is 3.5238 A, and that for CeO_2 (fluorite cubic, Z = 4) is 5.4110 A. When we calculate the diagonal array (R) between two lattices, then R = (5.411/3.5238) = 1.5356. If the two lattices are arrayed without changing at the interface, R is $\sqrt{2}$ = 1.4142. Therefore, when the two lattices interact with each other, we should consider the idea of molecular dynamics in which the adjacent lattices will be moved to lower the interface energy between layers at the interface. In this case, $\Delta R \approx \pm 4.3\%$. It could be expected that longer lattice (CeO_2) would be shortening and shorter lattice (Ni) would

be expanded to fit the condition. However, this lattice movement should occur at the first interface layer or two from the interface, but the more distant layers will retain their parameters. Therefore, it is important to choose the materials so as to match up the lattice parameters and thus allow the mechanical properties to be retained without failure during service. However, it is also very important to reduce the bandwidth in Fig 6 for overall development.

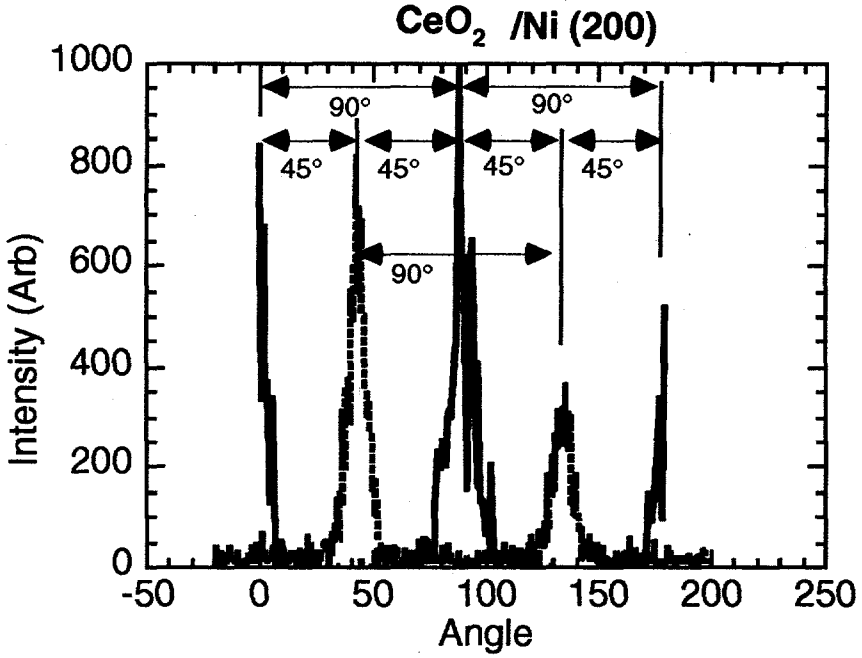

Fig. 6.
Two texture profiles obtained on cerium dioxide (200) deposited on textured Ni (200) and Ni itself.

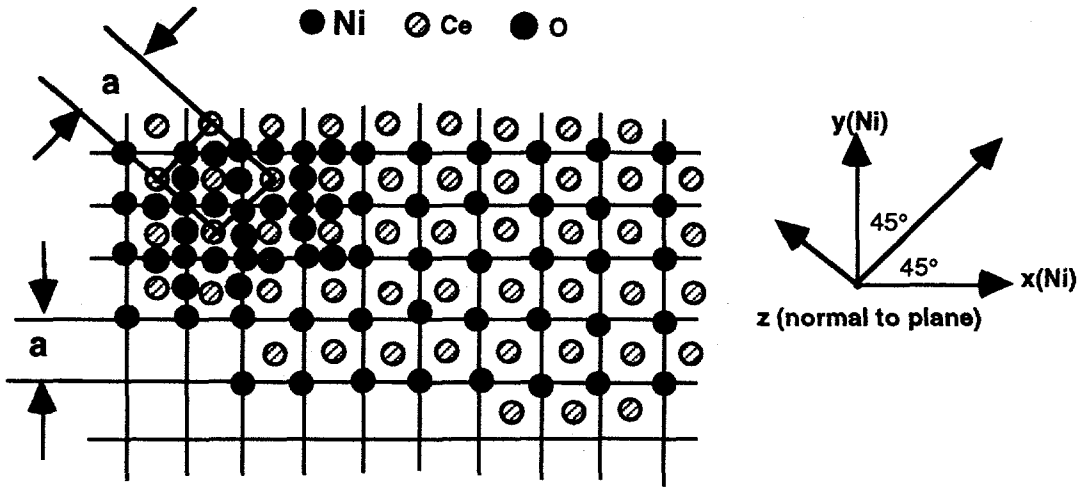

Fig. 7.
Schematic diagram of CeO_2 deposited on Ni. The lowest interface energy state between CeO_2 and Ni for both (200) could be 45° which is consistent with Fig. 6.

SUMMARY

Various coatings applications such as corrosion protection and electrical insulators and conductors are demonstrated as examples. The required conditions based on epitaxial relationships between interfaces and on thermodynamic/kinetic considerations for the development of surface modifications were demonstrated.

ACKNOWLEDGMENTS

This work has been supported by the U.S. Department of Energy, Advanced Research and Technology Development Fossil Energy Materials and Fusion Materials Program under Contract W-31-109-Eng-38. Drs. K. Natesan, D. L. Smith, H. D. You (ANL), W. Wiffen (USDOE), and Prof. W. D. Cho (Univ. of Utah) helped with discussions and with collaboration throughout this work.

REFERENCES

1. A. S. Nowick, "Nonstoichiometric perovskite as high-temperature protonic conductors," **Conference on Nonstoichiometric Ceramics and Intermetallics, Kona, HI, April 26-May 1, 1998.**

2. C. W. Tanner and A. V. Virkar, Instability of $BaCeO_3$ in H_2O-containing atmospheres, J. Electrochem. Soc. **143** (4) 1386-89 (1996).

3. S. Gopalan and A. V. Virkar, Thermodynamic stability of $SrCeO_3$ and $BaCeO_3$ using a molten salt method and galvanic cells, J. Electrochem. Soc. **140** (4) 1060-65 (1993).

4. J.–H. Park and W. D. Cho, *Fabrication of Intermetallic Coatings for Electrical Insulation and Corrosion Resistance on High-Temperature Alloys*, Surface Modification Technologies IX, T. S. Sudarshan, W. Reitz, and J. J. Stiglich, eds., The Minerals, Metals and Materials Society, Warrendale PA (1996), pp. 151–166.

5. L. B. Pfeil, "Improvements in Heat Resistant Alloys," Brit. Pat. No. 459848 (1937)

6. Park, J.-H., King, W. E., and Rothman, S. J., Cation grain-boundary diffusion in Cr_2O_3 and Cr_2O_3 doped with Y_2O_3, , J. Am. Ceram. Soc. **70**, 880 (1987).

7. C. Cotell, K. Przybylski, and G. J. Yurek, Proc. Symp. on Fundamental Aspects of High-Temperature Corrosion-II, D. A. Shores and G. J. Yurek, eds., Boston, May 4-9, 1986, The Electrochemical Society, Inc., Pennington, NJ, p. 103.

8. J.-H. Park and K. Natesan, Argonne National Laboratory Report ANL/FE-92/1 (1992).

9. J.-H. Park, ed., American Society of Metals (ASM), "*CVD-Film-Technology*" (in press, 1999).

10. J.-H. Park, and H. D. You, Unpublished work ANL (1997).